EPJ Web of Conferences **276**, 01025 (2023) https://doi.org/10.1051/epjconf/202327601025
SQM 2022

Exploration of the phase diagram within a transport approach

Olga Soloveva[1,2,*], *Pierre* Moreau[3], *Lucia* Oliva[2,4,5], *Taesoo* Song[9], *Ilia* Grishmanovskii[2], *Vadym* Voronuyk[1,8], *Viktar* Kireyeu[1,8], *Jörg* Aichelin[6,7], and *Elena* Bratkovskaya[9,1,2]

[1]Helmholtz Research Academy Hesse for FAIR (HFHF), GSI Helmholtz Center for Heavy Ion Physics, Campus Frankfurt, 60438 Frankfurt, Germany
[2]Institut für Theoretische Physik, Johann Wolfgang Goethe-Universität, Max-von-Laue-Str. 1, 60438 Frankfurt am Main, Germany
[3]Department of Physics, Duke University, Durham, NC 27708, USA
[4]Department of Physics and Astronomy "Ettore Majorana ", University of Catania, Via S. Sofia 64, I-95123 Catania, Italy
[5]INFN Sezione di Catania, Via S. Sofia 64, I-95123 Catania, Italy
[6]SUBATECH, University of Nantes, IMT Atlantique,IN2P3/CNRS 4 rue Alfred Kastler, 44307 Nantes cedex 3, France
[7]Frankfurt Institute for Advanced Studies, Ruth-Moufang-Strasse 1, 60438 Frankfurt am Main, Germany
[8]Joint Institute for Nuclear Research, Joliot-Curie 6, 141980 Dubna, Moscow region, Russia
[9]GSI Helmholtzzentrum für Schwerionenforschung GmbH, Planckstrasse 1, D-64291 Darmstadt, Germany

Abstract. We study equilibrium as well as out-of-equilibrium properties of the strongly interacting QGP medium under extreme conditions of high temperature T and high baryon densities or baryon chemical potentials μ_B within a kinetic approach. We present the thermodynamic and transport properties of the QGP close to equilibrium in the framework of effective models with N_f=3 active quark flavours such as the Polyakov extended Nambu-Jona Lasinio (PNJL) and dynamical quasiparticle model with the CEP (DQPM-CP). Considering the transport coefficients and the EoS of the QGP phase, we compare our results with various results from the literature. Furthermore, out-of equilibrium properties of the QGP medium and in particular, the effect of a μ_B- dependence of thermodynamic and transport properties of the QGP are studied within the Parton-Hadron-String-Dynamics (PHSD) transport approach, which covers the full evolution of the system during HICs. We find that bulk observables and flow coefficients for strange hadrons as well as for antiprotons are more sensitive to the properties of the QGP, in particular to the μ_B - dependence of the QGP interactions.

1 Introduction

It is known that the evolution of the deconfined QCD phase in ultra-relativistic heavy-ion collisions has been successfully described within hydrodynamic simulations and hybrid methods [1–4]. However, only a microscopic treatment can provide a proper non-equilibrium

*e-mail: soloveva@itp.uni-frankfurt.de

description of the entire dynamics through possibly different phases up to the final asymptotic hadronic states. Here we report on a recent progress made within the PHSD transport approach [5–9], which is an off-shell transport approach based on the Kadanoff-Baym equations in first-order gradient expansion. This approach sequentially describes the full evolution of relativistic heavy-ion collisions from the initial hard collisions and formation of strings, the deconfinement with a dynamic phase transition to a strongly interacting QGP, to hadronization and subsequent interactions in the expanding hadronic phase.
While the hadronic part is essentially equivalent to the conventional HSD approach [10], the microscopic properties of the QGP phase are described by the DQPM, which is based on the lQCD data and allows to interpret the equations of state (EoS) in terms of dynamical degrees of freedom and furthermore allows to evaluate the cross sections of the corresponding in/elastic reactions.The PHSD transport approach well describes observables from p+A and A+A collisions from SPS to LHC energies including electromagnetic probes [9].
In order to tackle the new challenge – i.e. the evolution of the partonic systems at finite μ_B – the PHSD approach has been extended to incorporate partonic quasiparticles and their differential cross sections that depend not only on T as in the previous PHSD studies, but also on μ_B explicitly [11]. Within this extended approach, the 'bulk' observables in HICs for different energies – from AGS to RHIC – for symmetric and asymmetric Au+Au/Pb+Pb collisions have been studied. Only a small influence of the μ_B modification of the parton properties (masses and widths) and their interaction cross sections has been found in bulk observables.

Furthermore, in Ref. [12] we extended our study to more sensitive observables, such as collective flow coefficients and a manifestation of the μ_B dependencies of partonic cross sections in the flow coefficients. In addition, we explore the relations between the in- and out-of equilibrium QGP by means of transport coefficients and collective flows.

2 Transport properties of the QGP at finite μ_B

We present transport coefficients of the QGP medium at finite μ_B where the phase transition is possibly changing from a crossover to a 1st order one. Due to the notoriuos difficulty for the estimation of transport coefficients at finite μ_B in lattice QCD it is necessary to resort to effective models which describe the chiral phase transition. It is important to note that while most of the models have a similar EoS, which agrees well with available lattice data, predictions for transport coefficients of the QGP can vary significantly already at $\mu_B = 0$ [11, 13–16].

In Refs. [15, 16] we have evaluated transport coefficients of the QGP medium for a wide range of μ_B for two models with a similar phase structure: the extended $N_f = 3$ PNJL model and the dynamical quasiparticle model with a hypothetical CEP (DQPM-CP) located at $\mu_B = 0.96$ GeV.
The shear and bulk viscosities for quasiparticles with medium-dependent masses $m_i(T, \mu_q)$ can be derived using the Boltzmann equation in the relaxation-time approximation (RTA) through the relaxation time:

$$\eta(T,\mu_q) = \frac{1}{15T}\sum_{i=q,\bar{q},g}\int\frac{d^3p}{(2\pi)^3}\frac{\mathbf{p}^4}{E_i^2}\tau_i(\mathbf{p},T,\mu_q)\times d_i(1\pm f_i)f_i, \tag{1}$$

$$\zeta(T,\mu_q) = \frac{1}{9T}\sum_{i=q,\bar{q},g}\int\frac{d^3p}{(2\pi)^3}\tau_i(\mathbf{p},T,\mu_q)\frac{d_i(1\pm f_i)f_i}{E_i^2}\left[\mathbf{p}^2 - 3c_s^2(E_i^2 - T^2\frac{dm_i^2}{dT^2})\right]^2, \tag{2}$$

where $q = (u, d, s)$, $d_q = 6$ and $d_g = 16$ are the spin and color degeneracy factors for quarks and gluons, respectively, whereas τ_i are the corresponding relaxation times. c_s is the speed of sound for fixed μ_B. The relaxation times are evaluated from the interaction rates by calculating the partonic differential cross-sections as a function of T and μ_B for the leading tree-level diagrams [11]:

$$1/\tau(p_i, T, \mu_q) = \Gamma_i^{on}(p_i, T, \mu_q) = \sum_{j=q,\bar{q},g} \int \frac{d^3 p_j}{(2\pi)^3} \, d_j \, f_j \, v_{rel} \int d\sigma_{ij\to cd}^{on} \, (1 \pm f_c)(1 \pm f_d), \quad (3)$$

where $v_{rel} = \frac{\sqrt{(p_i \cdot p_j)^2 - m_i^2 m_j^2}}{E_i E_j}$ denotes the relative velocity in the c.m. frame, d_j is the degeneracy factor for spin and color. The specific shear viscosity of the QGP matter is shown in Fig.

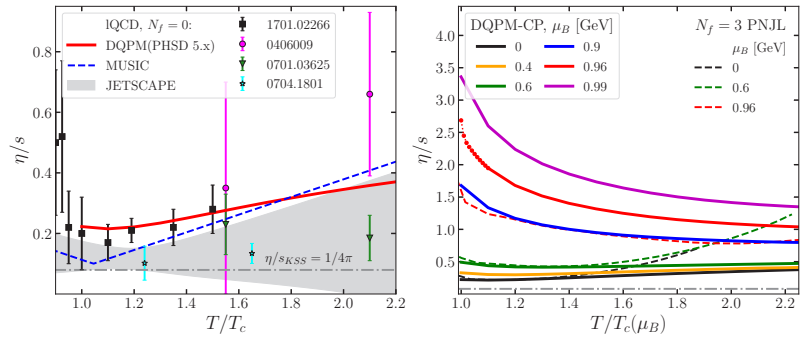

Figure 1. (Left) η/s as a function of T/T_c at $\mu_B = 0$. The symbols corresponds to the lQCD results for pure SU(3) gauge theory (black squares) [17], (green triangles and magenta circles) [18], (cyan stars) [19]. The red line corresponds to the DQPM results [16], while the dashed blue line displays the η/s parametrisation used in hydrodynamic simulations within MUSIC in [22]. The dash-dotted gray line demonstrates the Kovtun–Son–Starinets bound $(\eta/s)_{KSS} = 1/(4\pi)$ [20]. The grey area represents the model-averaged results from a Bayesian analysis of experimental heavy-ion data [21]. (Right) η/s as a function of $T/T_c(\mu_B)$ at finite μ_B: DQPM-CP results [16] (solid lines) are compared to the estimates from the $N_f = 3$ PNJL model (dashed lines) [15].

1 as a function of scaled temperature T/T_c at $\mu_B = 0$ (left) and at finite μ_B (right). At $\mu_B = 0$ we show results from the DQPM [16] (solid red line), in comparison with the lQCD results for pure SU(3) gauge theory [17–19], model-averaged results from a Bayesian analysis of the experimental heavy-ion data [21] (grey area) and η/s as employed in hydrodynamic simulations in [22] (dashed blue line). For finite $\mu_B \geq 0$ we compare the results from the PNJL and DQPM-CP models obtained by the RTA approach with the interaction rate. The estimates from both models show an increase of the specific shear viscosities η/s and electric conductivities σ_{QQ}/T with μ_B. While results for η/s are in agreement for moderate μ_B in the vicinity of the phase transition, there is a clear difference in σ_{QQ}/T essentially due to the different description of the partonic degrees of freedom [16].

3 Evolution of the QGP in the PHSD transport approach

To investigate the sensitivity of 'bulk' observables as well as flow coefficients of different hadrons produced in HICs to the modification of the partonic interactions and their transport

properties at non-zero baryon density we have considered the following two settings for the transport simulations:

- **PHSD5.0 -** $\mu_B = 0$ (dashed blue lines): the pole masses and widths of quarks and gluons depend only on T; however, the differential and total partonic cross sections are obtained by calculations of the leading order Feynman diagrams employing the effective propagators and couplings $g^2(T/T_c)$ from the DQPM at $\mu_B = 0$ [11]. Thus, the cross sections depend explicitly on the invariant energy of the colliding partons $\sqrt{s}$ and on T. This is realized in the PHSD5.x by keeping $\mu_B = 0$.
- **PHSD5.0 -** μ_B (solid red lines): the pole masses and widths of quarks and gluons depend on T and μ_B explicitly; the differential and total partonic cross sections are obtained by calculations of the leading order Feynman diagrams from the DQPM and explicitly depend on $\sqrt{s}$, T and μ_B. This is realized in the full version of PHSD5.x [11].

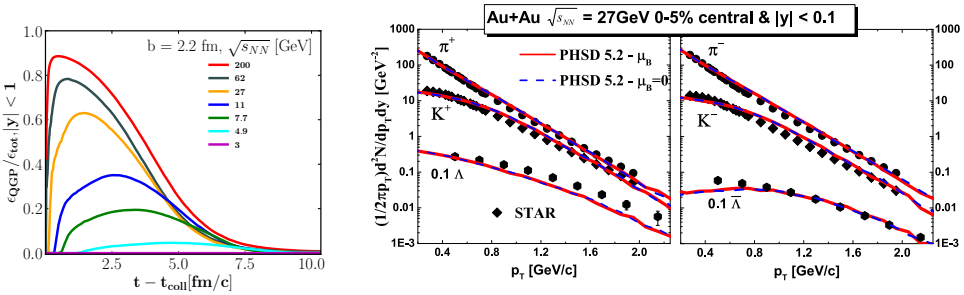

Figure 2. (Left) The QGP energy fraction from the PHSD as a function of time in central (impact parameter $b = 2.2$ fm) Au+Au collisions for different $\sqrt{s_{NN}} = 200 - 3$ GeV at the midrapidity region $|y| < 1$. (Right) The transverse momentum distributions for 0-5% central Au+Au collisions at $\sqrt{s_{NN}} =$ 27 GeV and midrapidity ($|y| < 1$) for PHSD5.2 with partonic cross sections and parton masses calculated for $\mu_B = 0$ (dashed blue lines) and with cross sections and parton masses evaluated at the actual μ_B in each individual space-time cell (solid red lines) in comparison to the experimental data from the STAR collaboration [23].

Fig. 2 (Left) displays the actual results for transverse momentum distributions for 0-5% central Au+Au collisions at $\sqrt{s_{NN}} = 27$ GeV and midrapidity ($|y| < 0.1$) for PHSD5.1 with partonic cross sections and parton masses calculated for $\mu_B = 0$ (dashed blue lines) and with cross sections and parton masses evaluated at the actual chemical potential μ_B in each individual space-time cell (solid red lines) in comparison to the experimental data from the STAR collaboration [23].

4 Summary

We find that HIC results from the extended PHSD transport approach, where in the QGP phase we found that transport coefficients have noticeable T and μ_B dependence, have been in agreement with the BES STAR data in case of bulk observables [11] and elliptic flow of charged particles [12], and reasonably agrees with the results from the hybrid approach [22]. It is important to note that, η/s used for hydrodynamic evolutions is close to the DQPM estimates as shown in Fig. 1 (left). However, results from the PHSD transport approach have shown a rather small influence of the μ_B-dependence of the QGP interactions on the elliptic flow than hybrid simulations. This small sensitivity of final observables

to the influence of baryon density on the QGP dynamics can be explained by the fact that at high energies, where the matter is dominated by the QGP phase, one probes the QGP at a very small μ_B, whereas at lower energies, where μ_B becomes larger, the fraction of the QGP drops rapidly (see Fig. 2 (left)). Therefore, the final observables for lower energies of order of $1 - 10$ GeV are in total dominated by the hadrons which participated in hadronic rescattering and thus the information about their QGP origin is washed out or lost.

The authors acknowledge inspiring discussions with W. Cassing, J. Torres-Rincon, C. Ratti. Furthermore, we acknowledge support by the Deutsche Forschungsgemeinschaft (DFG, German Research Foundation) through the grant CRC-TR 211 "Strong-interaction matter under extreme conditions" - project number 315477589 - TRR 211. I.G. also acknowledges support from the "Helmholtz Graduate School for Heavy Ion research". This work is supported by the European Union's Horizon 2020 research and innovation program under grant agreement No 824093 (STRONG-2020) and by the COST Action THOR, CA15213. The computational resources have been provided by the Goethe-HLR Center for Scientific Computing.

References

[1] H. Song and U. W. Heinz, Phys. Rev. C **78** (2008), 024902
[2] C. Shen, Z. Qiu, H. Song, J. Bernhard, S. Bass and U. Heinz, Comput. Phys. Commun. **199** (2016), 61-85
[3] I. A. Karpenko, P. Huovinen, H. Petersen and M. Bleicher, Phys. Rev. C **91** (2015) no.6, 064901
[4] G. S. Denicol, C. Gale, S. Jeon, A. Monnai, B. Schenke and C. Shen, Phys. Rev. C **98** (2018) no.3, 034916
[5] W. Cassing and E. L. Bratkovskaya, Phys. Rev. C **78** (2008), 034919
[6] W. Cassing, Eur. Phys. J. ST **168** (2009), 3-87
[7] W. Cassing and E. L. Bratkovskaya, Nucl. Phys. A **831** (2009), 215-242
[8] E. L. Bratkovskaya, W. Cassing, V. P. Konchakovski and O. Linnyk, Nucl. Phys. A **856** (2011), 162-182
[9] O. Linnyk, E. L. Bratkovskaya and W. Cassing, Prog. Part. Nucl. Phys. **87** (2016), 50-115
[10] W. Cassing and E. L. Bratkovskaya, Phys. Rept. **308** (1999), 65-233
[11] P. Moreau, O. Soloveva, L. Oliva, T. Song, W. Cassing and E. Bratkovskaya, Phys. Rev. C **100** (2019) no.1, 014911
[12] O. Soloveva, P. Moreau, L. Oliva, V. Voronyuk, V. Kireyeu, T. Song and E. Bratkovskaya, Particles **3** (2020) no.1, 178-192
[13] R. Marty, E. Bratkovskaya, W. Cassing, J. Aichelin and H. Berrehrah, Phys. Rev. C **88** (2013), 045204
[14] J. Grefa, M. Hippert, J. Noronha, J. Noronha-Hostler, I. Portillo, C. Ratti and R. Rougemont, Phys. Rev. D **106** (2022) no.3, 034024
[15] O. Soloveva, D. Fuseau, J. Aichelin and E. Bratkovskaya, Phys. Rev. C **103** (2021) no.5, 054901
[16] O. Soloveva, J. Aichelin and E. Bratkovskaya, Phys. Rev. D **105** (2022) no.5, 054011
[17] N. Astrakhantsev, V. Braguta and A. Kotov, JHEP **04** (2017), 101
[18] A. Nakamura and S. Sakai, Phys. Rev. Lett. **94** (2005), 072305
[19] H. B. Meyer, Phys. Rev. D **76** (2007), 101701
[20] P. Kovtun, D. T. Son and A. O. Starinets, Phys. Rev. Lett. **94** (2005), 111601

[21] D. Everett *et al.* [JETSCAPE], Phys. Rev. Lett. **126** (2021) no.24, 242301
[22] C. Shen and S. Alzhrani, Phys. Rev. C **102** (2020) no.1, 014909
[23] L. Adamczyk *et al.* [STAR], Phys. Rev. C **96** (2017) no.4, 044904